

TJ25.1 NWS Southern Region Numerical Optimization and Sensitivity Evaluation in Non-Stationary SWAN Simulations

Alex Gibbs
Forecaster
11691 SW 17th Street
Miami, FL, 33165
Alex.Gibbs@noaa.gov

Pablo Santos
Meteorologist In Charge
11691 SW 17th Street
Miami, FL, 33165
Pablo.Santos@noaa.gov

André van der Westhuysen
UCAR at NOAA/EMC/MMAB
Camp Springs, MD
Andre.VanderWesthuysen@noaa.gov

Roberto Padilla-Hernandez
IMSG at NOAA/EMC/MMAB
Camp Springs, MD
Roberto.Padilla@noaa.gov

1. INTRODUCTION

New features have been introduced to the National Weather Service Southern Region (NWSSR) SWAN model configuration (Settelmaier et al., 2011) with an emphasis on improving numerical accuracy based on a series of sensitivity and validation tests over shallow water regions with complex coastlines. This system is serving also as the basis of the future Nearshore Wave Prediction System (NWPS), which is being developed through the National Oceanic and Atmospheric Administration (NOAA)'s Operations and Services Improvement Process (OSIP). The objective is to baseline NWPS in the second-generation Advanced Weather Interactive Processing System (AWIPS II), to be rolled out to Weather Forecast Offices (WFOs) in the near future.

Those tests involved different flow regimes across fetch and depth-limited waters and two real-time hindcast scenarios that include Hurricane Irene (2011) evaluated over the Gulf Stream waters of South Florida and the 1993 Superstorm over the Gulf of Mexico. Each test included comparisons between the model output considering various source term integration time steps, directional resolutions and single to multiple iterations per time step.

In this paper the tests and results upon which model optimization and operational setting was based are described. The structure of the paper is as follows: A brief description of the SWAN model is presented in section 2. The sensitivity tests are discussed in section 3, with conclusions at the end of each set of tests. The final conclusions of this study are provided in section 4.

2. MODEL DESCRIPTION

The SWAN model (Booij et al., 1999) is a third-generation wave model that was developed to estimate wave conditions in small-scale, coastal regions with shallow water, (barrier) islands, tidal flats, local wind, and ambient currents. This model was developed and is being maintained by the Delft University of Technology (The SWAN Team, 2010a,b).

The SWAN model accounts for wave propagation and wave growth and decay from deep to shallow water by solving the wave action balance equation:

$$\frac{\partial}{\partial t} N + \frac{\partial}{\partial x} c_x N + \frac{\partial}{\partial y} c_y N + \frac{\partial}{\partial \sigma} c_\sigma N + \frac{\partial}{\partial \theta} c_\theta N = \frac{(S_{wind} + S_{nl} + S_{wc} + S_{bot} + S_{brk})}{\sigma} \quad (1)$$

The first term on the left-hand side represents the local rate of change of action density in time, the second and third terms represent propagation of action in geographical x, y space, respectively (with propagation velocities c_x and c_y). The fourth term represents shifting of the relative frequency due to variations in depths and currents (with propagation velocity c_σ in σ or frequency space). The fifth term represents depth and current induced refraction (with propagation velocities c_Θ in Θ space). The growth and decay of the wave field are described by various source terms, including (right-hand side of the equation): wind input (S_{wind}), nonlinear wave-wave interactions (S_{nl}), whitecapping (S_{wc}), bottom friction (S_{bot}) and depth-induced breaking (S_{brk}), where each contribute to the processes that evolve as waves transition from deep to shallow water and/or are locally generated. For more details, see Booij et al. (1999).

The action balance equation (1) has been implemented in SWAN using implicit propagation schemes in geographical space and semi-implicit propagation schemes in spectral (frequency and direction) spaces. This, in principle, allows the model to remain stable even with large time steps that violate the Courant-Friedrichs-Levy (CFL) stability criterion. However, some source terms, in particular the nonlinear S_{nl} term, have very short time scales of change at high frequencies. Unless very small source term integration time steps are applied, the solution rapidly becomes inaccurate and unstable. To achieve physically realistic numerical solutions within the context of operationally applicable computational times (i.e. economical time steps), many third-generation wave models, including SWAN, utilize an action density limiter. This limiter restricts the change in action density within the time step or iteration, thereby maintaining a stable solution during source term integration. Properly applied, this limiter does not significantly affect the solution in SWAN (Zijlema and Van der Westhuysen, 2005).

However, this limiter could unintentionally suppress changes in the wave spectrum in non-stationary mode if a relatively large computational time step would be used. This is manifested, for example, as a lag in wave growth during strongly forced conditions. This was first noted by Fraza (1998), who proposed to reduce the negative influence of the limiter by performing one or more iterations of the semi-implicit source term integration per time step. This provides an alternative that may be more economical than the simple application of a shorter time step. For more information regarding action density limiters used in third-generation wave models and the use of the propagation scheme mentioned, refer to Tolman (2002), WAMDI Group (1988), Hersbach and Janssen (1999), and Zijlema and Van der Westhuysen (2005).

These considerations are very relevant to local high-resolution wave modeling efforts at NWSSR WFOs, where the use of relatively small time steps are not economically feasible for operational implementation, considering the model platform provided. Therefore, a variety of operational model configurations featuring various computational time steps and spectral resolutions were tested and compared, the results of which are discussed in this paper.

3. NUMERICAL OPTIMIZATION AND SENSITIVITY TESTS

One of the critical topics addressed with the deployment of the SWAN model to the 13 NWSSR coastal WFOs (Settelmaier et al., 2011), and for the future national NWPS deployment, was to optimize the numerical settings of the model, yet remain operationally achievable with regard to the computational expense. To achieve this goal, a series of numerical sensitivity tests were conducted.

First, 16 idealized simulations over the northeast Gulf of Mexico and the Miami, South Florida region, were evaluated in nonstationary mode on a rectangular computational grid.

These tests were carried out to evaluate the impact of numerical settings on wave growth during rapidly changing wind conditions. To isolate the wave generation process, these idealized cases did not include any boundary conditions, currents or water level variations. The spatial grid discretization in these tests was $\Delta x = \Delta y = 1800$ m, and the frequency range was from 0.05 to 1.0 Hz. A number of alternatives were tested for the directional distribution and time stepping: 24, 31 and 36 directional bins ($\Delta\theta = 15^\circ, 12^\circ$ and 10°), and time steps of 300-1800s, along with single to multiple iterations per time step.

Subsequently, two realistic field cases were considered. First, a hindcast simulation of Hurricane Irene (2011) was conducted, using the aforementioned South Florida domain and range of numerical settings. This case included boundary conditions from NOAA/NWS/NCEP's operational WAVEWATCH III® (WW3) model, the official National Digital Forecast Database (NDFD) wind forecast from WFO Miami, Florida and current fields from NCEP's Real-Time Ocean Forecast System (RTOFS-Atlantic). The second field case was the 1993 Superstorm over a large grid on the scale of the Gulf of Mexico. The primary forcing in this latter case was the wind field over the Gulf region, with boundary conditions, currents and water levels being excluded.

3.1 Idealized Case

The northeast Gulf of Mexico domain is suitable for simple numerical tests over depth and fetch-limited waters (Figure 1). The bottom topography is characterized by very broad shelves and flat bottom profiles across the Apalachee Bay Region (eastern half of the domain). However, south of the Florida Panhandle (western half of the domain), steeper profiles are encountered due to the large Desoto Canyon extending north toward the coast from Panama City to Pensacola. To resolve these bathymetric complexities, the three arc-second gridded database (Coastal

Relief Model – CRM), available at NOAA's the National Geophysical Data Center (NGDC) was implemented for the test.

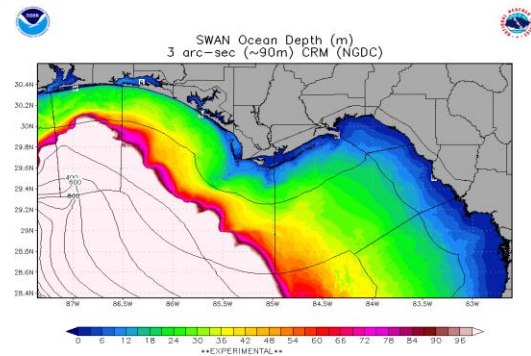


Figure 1: Bathymetry for the Northeast Gulf of Mexico, derived from the three arc-second (~90 m) gridded data from the Coastal Relief Model (NOAA NGDC, 2011).

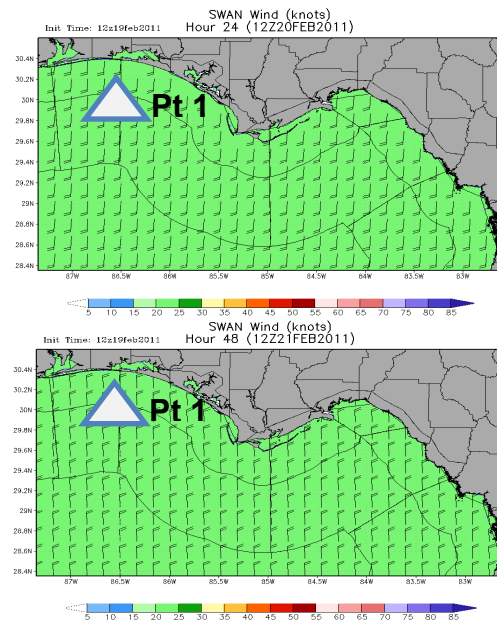


Figure 2. Synthetic wind field featuring southerly winds of $U_{10} = 10 \text{ ms}^{-1}$ (20 knots) through the initial 24 hours (top), followed by northerly winds from hours 30-48 (bottom). Included is output point “Pt. 1”.

3.1.1 Wind

A synthetic wind field out to 48 hours was used as forcing in these tests. It was configured with a southerly wind of $U_{10} = 10 \text{ ms}^{-1}$ through

the initial 24 hour period, followed by a quick transition between hours 24 through 30 to a south to north wind, then a northerly component at the same magnitude from hours 30 through 48 (Figure 2).

3.1.2 Significant Wave Height

Figures 3 and 4 show time series results of the significant wave height H_s at an output point Pt. 1, south of Destin, Florida (Fig. 2) from six different simulations. For this particular point, the initial wave growth out to 24 hrs was caused by a southerly wind of $U_{10}=10 \text{ ms}^{-1}$ at a fetch of approximately 190 km (102.5 nm), extending north from the southern grid boundary to Pt. 1. The depth at the point is approximately 50 m, which is within the transition zone between the deep waters at the northern tip of the Desoto Canyon and the Panhandle shelf waters (surf zone) as shown in Fig. 1. Simulations with three different time steps ($\Delta t=1800, 900$ and 600 s) were compared, with the main focus on the initial 24 hours up to the point, where a fetch-limited state was reached. Figure 3 shows the results for three different time steps, with a maximum number of iterations per time step set to 1. Considerably different response times in wave growth were observed between the various simulations. For instance, the 1800 s solution was only 50% of the much more responsive 600 s solution during the initial 24 hour growth phase.

Figure 4 shows the results of similar simulations, but now with the maximum iteration increased to 3 per time step. The lag in wave growth was reduced significantly when compared to the simulations in Fig. 3, particularly for the larger integration time steps (900 s and 1800 s). Similar differences are also found on the tail of the 48 hr simulation, as the H_s begins to decrease due to the combination of the rapid wind shift from south to north and the decreased fetch over shallow waters extending south from the coast to Pt. 1.

3.1.3 Test Conclusions

The results from this case over the northeast Gulf of Mexico indicate that reducing the model time step and/or increasing the maximum number of iterations at each time step, correspondingly, allows the model to arrive at the desired solution and converge much more quickly during rapidly changing wind conditions. For this case, the directional increase in resolution from 24 to 36 bins did not appear to have much effect in terms of model response time (not shown). However, it increased the overall computational time by a factor of 1.17 to 1.35. Further testing at points in shallower waters in areas with higher wave refraction combined with lower frequencies

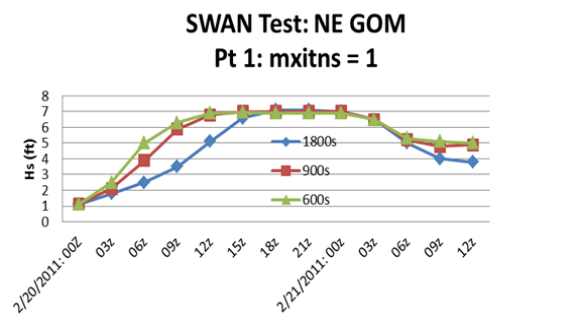


Figure 3. Comparison of H_s time series of SWAN results between three different source time steps ($\Delta t=1800, 900$, and 600 s) at Pt. 1 with a maximum number of iterations per time step of 1.

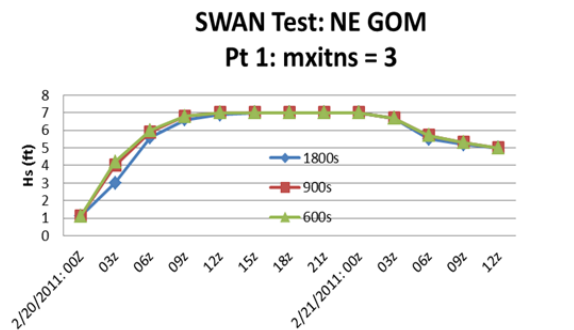


Figure 4. As in Fig. 3, but with a maximum number of iterations per time step of 3.

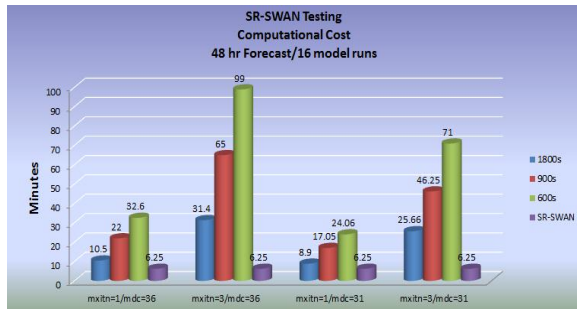


Figure 5. Comparison between the computational expense of three directional resolutions and three computational time step alternatives. The number of directional bins is indicated by mdc and maximum iterations per time step by mxitn. SR-SWAN results (purple) feature a mxitn of 1, a mdc of 24 and a computational time step of 1800 s.

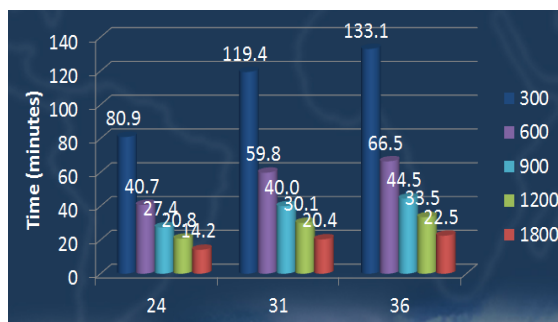


Figure 6. Comparison between computational expense of three directional resolutions (24, 31 and 36 bins) and five computational time step alternatives configured at the NWS WFO Miami, Florida. Iterations per time step were set to 1.

would most likely yield greater or more noticeable differences between 24, 31 and 36 directional bins.

Figure 5 illustrates the overall computational expense between the 16 different simulations. These tests were performed on a dual quad core (8 core/64 bits) Intel Xeon (T5500) machine with 24 GB of RAM and a processor speed of 2.4 GHz. The number of grid points in these simulations was 280 x 134 with a total equal to 37,520 grid points.

Similar simulations using a nearly identical platform were evaluated over the South Florida coastal waters at NWS WFO Miami. The main difference compared to the northeast Gulf of Mexico simulations was the domain size, which resulted in different computational times, even though the numerics tested within the model runs were the same. The number of grid points in the Miami simulations was 289 x 222 with a total equal to 64,158. Results, however, remained consistent with regard to the model tendencies listed above (Figure 6).

3.2 Hurricane Irene (2011) Field Case

The same approach and methods previously discussed in the idealized case across the northeast Gulf of Mexico were implemented in a real-time event that occurred across the Gulf Stream waters of South Florida as Hurricane Irene was passing from south to north across the northern Bahamas, east of the Florida Peninsula, from August 25-29, 2011 (Figure 7). Boundary conditions from NOAA/NWS/NCEP’s operational WW3 (forced by GFDL hurricane model) and currents from NCEP’s RTOFS-Atlantic were included in these simulations. Multiple model time steps, a constant directional resolution of 24 and only one iteration per time step were included in these simulations.

Since observations in this region were sparse, results were evaluated at two NDBC stations along with one arbitrarily defined point near the center of the model grid (Figure 8). NDBC station 41114 (Pt. 1) is located near Fort Pierce, Florida with a water depth of 16.15 m (52.98 ft), in the vicinity of a very sharp bathymetry gradient extending shoreward of its location. Station 41114 was the only location with wave measurements within this domain. Since it lies on the domain boundary, it effectively serves to evaluate the quality of the incoming WW3 boundary conditions, as shown below. Wind observations at Settlement Point on the western edge of Grand Bahama Island

(Pt. 3) were archived, which was a desirable location considering the proximity to the

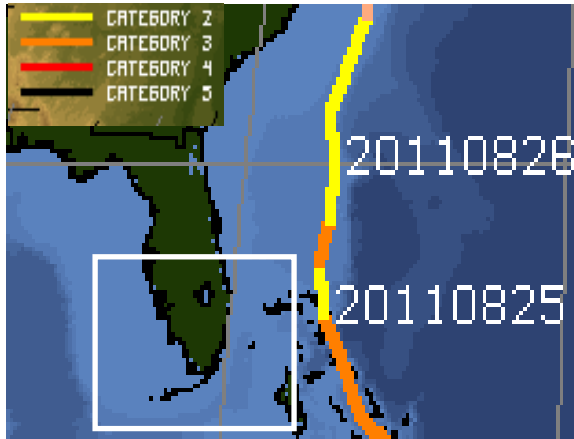


Figure 7. Track and intensity of Hurricane Irene as it passed east of the Florida Peninsula on August 25 and 26th of 2011. The orange track indicates Irene was a Category 3 Hurricane and the yellow a Category 2 Hurricane. The white box describes the modeled domain configured for the tests.

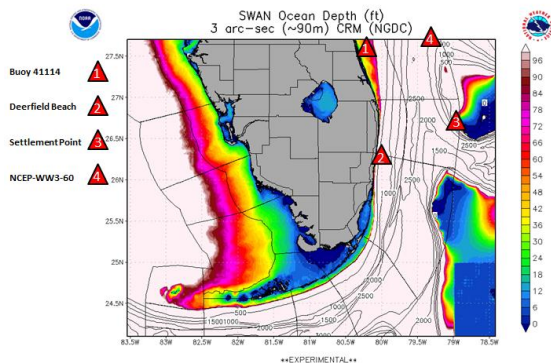


Figure 8: Bathymetry (NOAA NGDC, 2011) of the South Florida model domain with the four output stations (triangles numbered 1 through 4).

tropical cyclone passing to the east. Deerfield Beach (Pt. 2) was an arbitrarily defined point located near the center of the model grid. This point was selected due to its geographical location and distance away from the domain grid boundaries, to minimize the dominance of the boundary conditions on the numerical sensitivity results.

3.2.1 Wind

The official gridded wind forecast derived within the Interactive Forecast Preparation System - Graphical Forecast Editor (IFPS-GFE) from NWSSR WFO Miami was used during these simulations as forcing (Figure 9). In addition, these winds reflect the official National Hurricane Center (NHC) track of Irene during this period, which included the 34, 50 and 64 knot wind radii.

The initial 24 hrs of the forecast depicts primarily north-northwest flow gradually backing toward the west as Irene began to pull north of the computational model grid. The 34 knot wind radii clipped the critical offshore marine waters east of West Palm Beach near the northern Bahamas. As a result, a Tropical Storm Warning was issued during this time over these marine areas. The 64 knot wind radii can be tracked along the northeastern side of the open grid boundary out through hour 12 within these runs.

Although Irene quickly began to lift north and away from the South Florida after the initial 24 hr period (Figs. 7 and 9), a large amount of long-period energy out of the north and northeast continued to impact the model simulations due to a large fetch - see the 25 km Advanced Scatterometer (ASCAT) pass in Figure 10. Favorable Tropical Storm winds at this point extended outward across the northwest quadrant of Irene to approximately 275 km from the storm center, which continued to drive north and northeast energy south across the South Florida Atlantic waters.

Wind observations from Settlement Point (Pt. 3 in Fig. 8) were used to assess the accuracy of the official wind forecast used as forcing in the SWAN simulations. Figures 11-14 illustrate these comparisons and the overall forecast bias with respect to wind direction and speed at this point. They show a good correlation between the observations at Settlement Point with only a 1.18 ms^{-1} bias for wind speed and

approximately a five degree bias for wind direction.

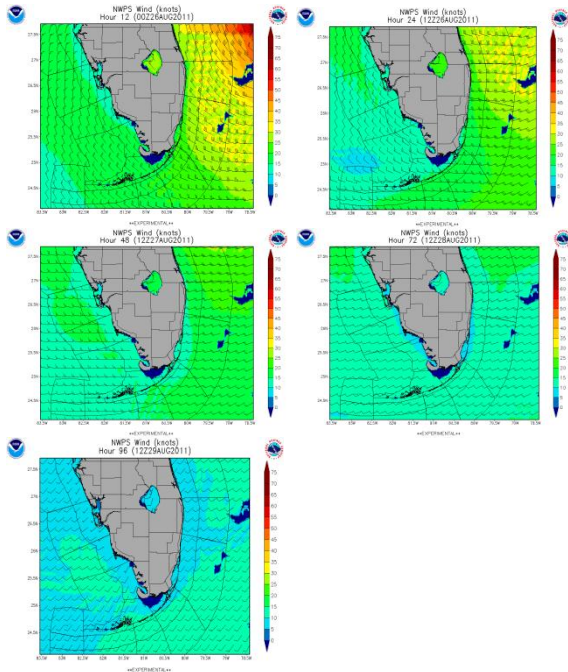


Figure 9. Snapshots of the winds utilized in these 96 hr SWAN hindcast simulations.

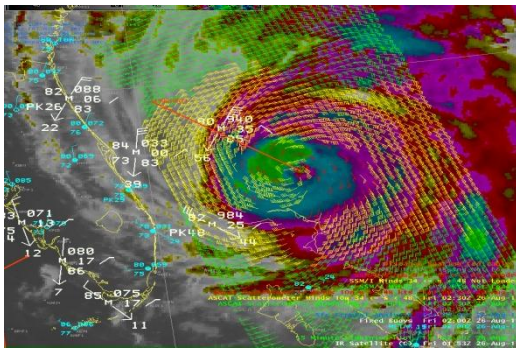


Figure 10. Infrared satellite imagery on Friday the 26th of August at 0153z. Overlaid, is a 25 km ascending Advanced Scatterometry (ASCAT) pass and buoy observations plotted revealing the very broad tropical storm wind radii extending outward from the storm center.

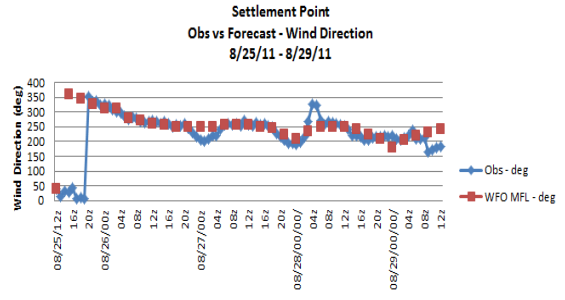


Figure 11. Time-series comparison of wind direction. Observations against the official forecast at Settlement Point (Pt. 3), for August 25-29, 2011.

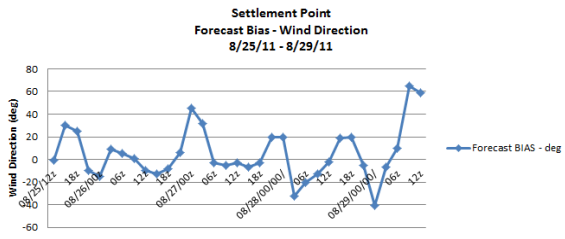


Figure 12. Forecast bias, or error, for the wind direction at Settlement Point (August 25-29, 2011). The average error or bias over the time range depicted was 5.09 degrees.

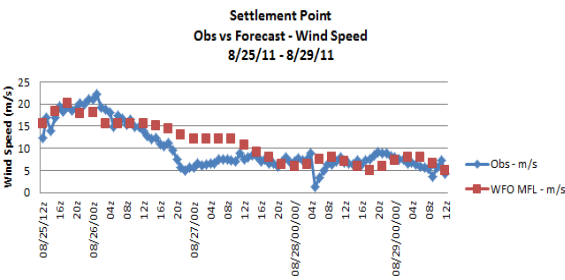


Figure 13. Time-series comparison of wind speed. Observations against the official forecast at Settlement Point (Pt. 3), for August 25-29, 2011.

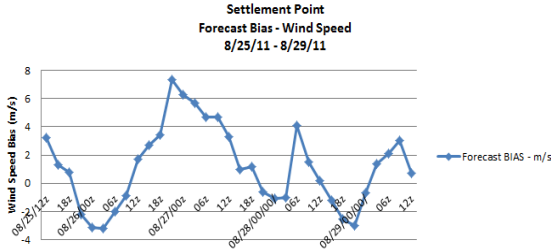


Figure 14. Forecast bias, or error, for the wind speed at Settlement Point (August 25-29, 2011). The average error or bias over the time range depicted was 1.18 m s^{-1} .

3.2.2 Significant Wave Height results

Figures 15-21 show a time series of the significant wave height H_s and associated errors at stations 41114 near Fort Pierce (Pt. 1) and Deerfield Beach (Pt. 2) as Irene was passing to the east. Comparisons between multiple model time steps ranging from 150s to 1800s were evaluated, while keeping the maximum number of iterations per time step at 1.

For these particular points of interest, wave growth during the initial 12 to 24 hr period was caused by a combination of north and northwest wind in the range of $U_{10}=10\text{-}15 \text{ ms}^{-1}$ and the incoming energy, input from the multi-gridded WW3 defined spectral points (used to initialize the grid boundaries), propagating south toward the station. Buoy 41114's general vicinity to the northern grid boundary was primarily influenced by the WW3 spectral input, which resulted in very little, if any, identifiable spread between the various time step solutions evaluated (Fig. 15).

The average error or bias between the smallest time step solution of 150 s (Fig. 16) and the observations was 0.26 ft (0.08 m) over the entire 96 hr time series of the simulation. However, an error or bias as high as 3.73 ft (1.14 m) over the initial 54 hrs (critical period of interest), where the rate of change in wave growth was at a maximum, revealed an over-forecasted solution (Fig. 17). This is likely due to

inaccuracies in the WW3 forecast, considering the vicinity of the model boundary to this point. A stronger than observed wind forecast is another potential source of error. However, observations from across the area indicate wind forecast errors were generally small or similar to those in Figs. 11-14.

The time series results at Deerfield Beach (Pt. 2) revealed the expected range in wave growth rates between the simulations with time steps ranging from 1800 s to 150 s, with the 1800 s simulation displaying the greatest lag (Figs. 18 and 19). Since there was no observation for this point, the average difference (Figs. 20 and 21) between the 1800 s and 150 s solutions was calculated yielding -0.24 ft (-0.07 m) with a maximum difference of -3.9 ft (-1.18 m). The negative bias indicates that the 1800 s time step solution consistently under-predicted the H_s compared to the 150 s solution during the critical period of interest (initial 54 hrs) where the maximum rate of wave growth occurred.

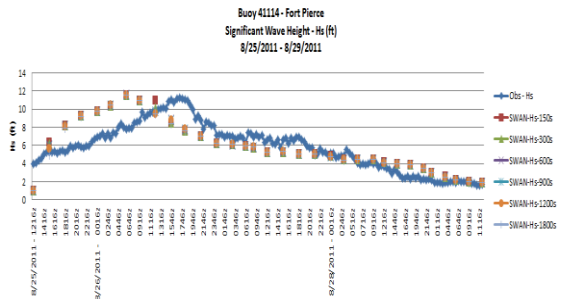


Figure 15. H_s time series of the SWAN model results between multiple computational time steps at station 41114 (Pt. 1) compared to the observations.

3.2.3 Test Conclusions

Results revealed a strong correlation between the wind forecasts and observations from the time series at Settlement Point. Simulation results at NDBC station 41114 revealed that during the early part of the forecast, the predicted H_s had a strong positive bias. This was

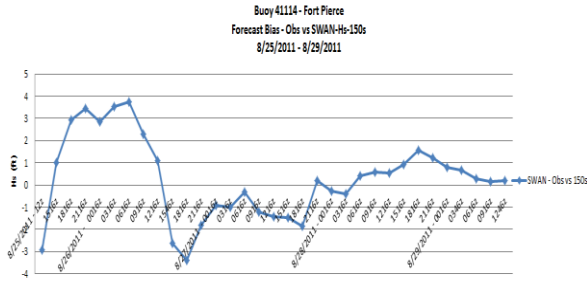


Figure 16. Forecast bias, or error, for H_s at station 41114 (Pt. 1), for August 25-29, 2011. The average error or bias over the time range depicted was 0.26 ft (0.08 m) over the entire series.

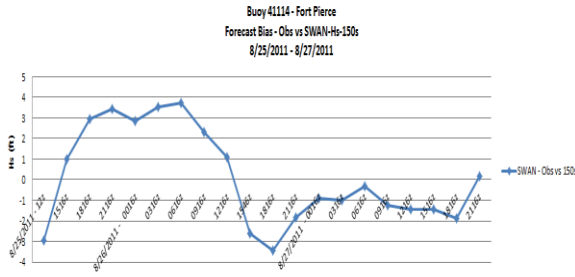


Figure 17. Detail of Fig. 16 for August 25-27, 2011) showing a maximum error of 3.73 ft (1.14 m) over the initial 54 hrs.

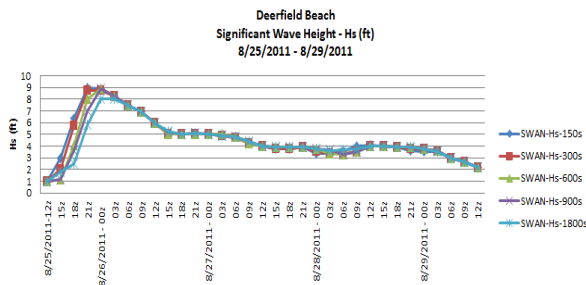


Figure 18. H_s time series of the SWAN results between multiple source time steps at Deerfield Beach (Pt. 2).

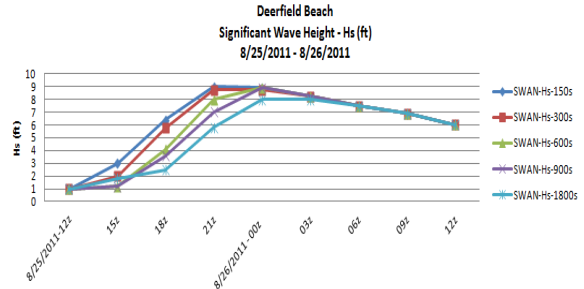


Figure 19. As Fig. 18, but for the initial 54 hrs of the runs.

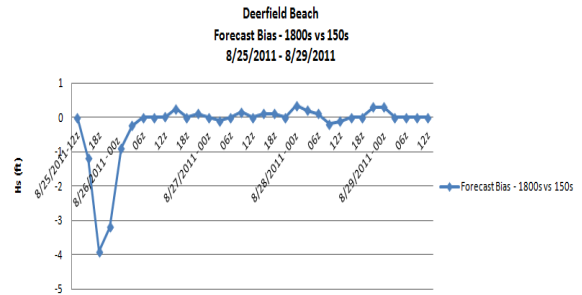


Figure 20. Forecast difference for SWAN- H_s 1800 s vs SWAN- H_s 150 s at Deerfield Beach (Pt. 2), August 25-29, 2011.

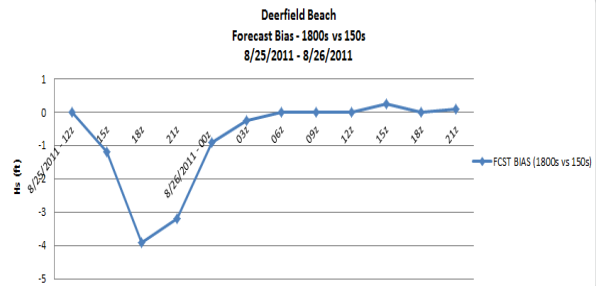


Figure 21. As Fig. 20, but for the initial 54 hrs of the runs.

most likely due to the quality of the WW3 forecast, which has a dominant influence at this location. Farther south along the coast and away from the grid boundary, at the defined Deerfield Beach point, considerable spread was found between the various time steps during the critical period of interest where the maximum rate of wave growth occurred. This is in line with the results of the idealized tests considered above. However, without

observations to compare against, there was no conclusive evidence of which time step was the optimal solution at this point.

3.3 Superstorm 1993 Field Case

The final case considered is the March 12-14, 1993 Superstorm (Settelmaier et al., 2011). Similar to the Irene case, multiple model time steps were compared against observations across the Gulf of Mexico, while keeping 24 directional bins and a maximum number of iterations per time step of 1.

The primary forcing in these simulations was generated by the Advanced Research WRF (ARW) model, which was initialized by the North American Regional Reanalysis (NARR) data. A gridded spatial resolution of 12 km was used over the Gulf of Mexico and portions of the East Coast. These runs did not account for wave-current interactions and were primarily forced by the wind output from the NARR/WRF simulations. Bathymetry over the region was derived from the one minute (~1.8 km) gridded database (ETOPO1) provided by NGDC. Wave observations were obtained at two buoy stations located over water depths ranging from 3000 to 3500 m (Figure 22). For more details refer to Settelmaier et al. (2011).

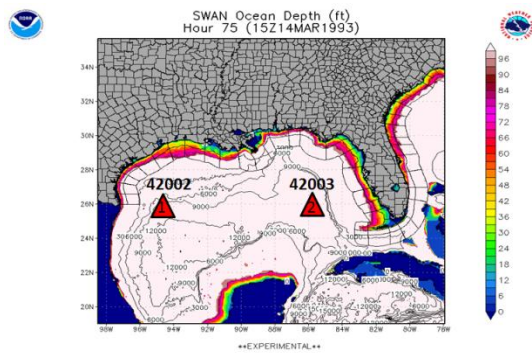


Figure 22. Bathymetry of the Gulf of Mexico and the U.S. Southeast coast with the two evaluated stations (triangles numbered 1 and 2).

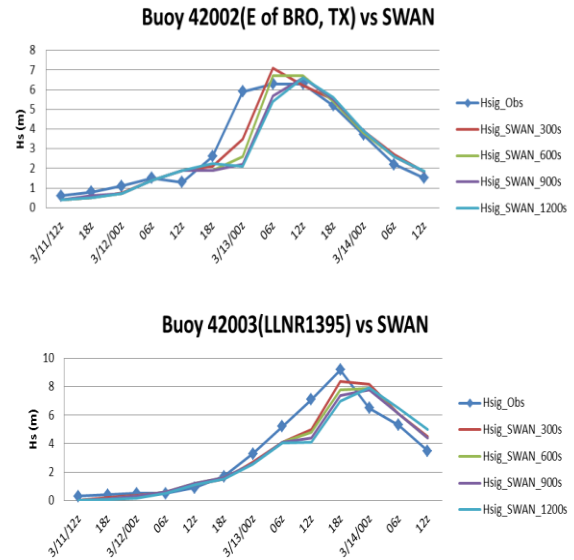


Figure 23. Comparison between the H_s time series of SWAN simulations featuring various computational time steps, and observations at NDBC stations 42002 and 42003.

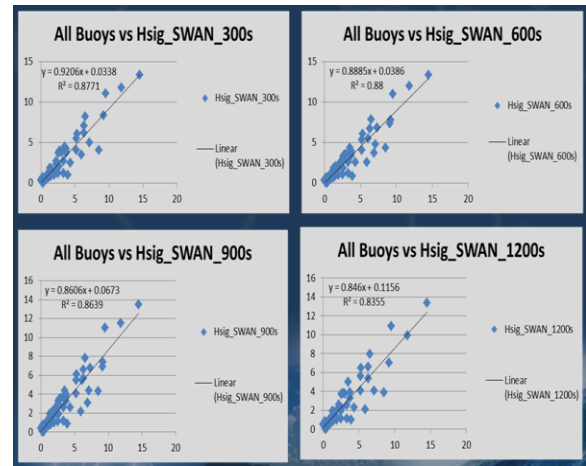


Figure 24. Comparison of SWAN results for simulations with various time steps and observations at stations 42002 and 42003 in Fig. 22. These plots also include results from stations 41009 (off the East Central Florida coast) and 41002 (off the mid Atlantic coast) not shown in Fig. 22. Included are linear regression fits, with a positive correlation coefficient ranging from 0.83 to 0.88.

3.3.1 Significant Wave Height

Figure 23 compares the H_s time series results of simulations with computational time steps ranging from 300 s to 1200 s with observations at NDBC stations 42002 and 42003 in the Gulf of Mexico during this event. The time series show that the observed maximum rate of wave growth that occurred through the second half of the simulations increased much more quickly than all of the SWAN solutions, which led to an overall under-forecasted event by the model, particularly during the period when conditions changed the fastest. However, the 300-600 s time step options revealed the most accurate solutions, with the main emphasis on the second half of the time series as the strong frontal system quickly traversed the domain from west to east. Figure 24 illustrates an overall strong linear relationship with a positive correlation coefficient ranging from 0.83 to 0.88 for all time steps and overall show a tendency of improving accuracy with decreasing time steps. These regression analyses in Fig. 24 include also NDBC stations 41009 and 41002 within the domain near the eastern side of the grid or off the east coast, which demonstrated very similar results as the two stations discussed in this paper.

3.3.2 Test Conclusions

The sensitivity tests for this field case showed the 300-600 s time step simulations to be the most accurate, in particular during the initial strong growth phase at the onset of the event. It is noted, however, that none of the SWAN simulations captured the rapid increase in significant wave height during this period very well. Nonetheless, taken over the entire event, satisfactory correlation coefficients are found between the SWAN results and observations.

4. CONCLUSIONS

Results suggest that the most operationally effective adjustment in trying to numerically

optimize the NWSSR SWAN (and future NWPS) was the use of a smaller computational time step to improve the model response time during rapidly evolving high-end marine events. Striking a compromise between the model platform and the computational expense on the one hand, and accuracy on the other, it was decided to reduce the model time step to 600 s with a directional resolution of 24 bins and remaining with 1 iteration per time step. However, the Hurricane Irene and Superstorm 1993 cases (Figs. 19 and 23) revealed that for extreme events smaller time steps such as 300 s at the very least are a better choice. Under normal operational conditions, 600 s appears to be an acceptable compromise.

Although a 600 s time step still violates the CFL criterion as discussed in section 2 (provided a grid increment of 1800 m at each forecast site), the combination of the action density limiter and the propagation scheme used in SWAN allows for a verifiable and more economical operational configuration. To compensate for the overall increased computational expense with this adjustment (from the original 1800 s time step when SWAN was first deployed across NWSSR), the SWAN hot start option was activated and implemented at each NWSSR coastal WFO which will also be included with NWPS. This additional feature allows the forecaster the option to define the initial conditions based on the previous run and to eliminate the necessary model spin-up period that is required with nonstationary compute mode.

5. REFERENCES

- Booij, N., Ris, R.C., Holthuijsen, L.H., 1999. A third-generation wave model for coastal regions: 1. Model description and validation. *J. Geophys. Res.*, **104** (C4), 7649–7666.
- Fraza, L. A. J., 1998: Testing the non-stationary option of the SWAN wave model. M.Sc. thesis, Delft University of Technology, 47 pp.

Hersbach, H., Janssen, P.A.E.M., 1999: Improvement of the short-fetch behavior in the wave ocean model (WAM). *J. Atmos. Ocean. Technol.*, **16**, 884-892.

NOAA National Geophysical Data Center (NGDC), cited 2011: U.S Coastal Relief Model (CRM). [Available online at <http://www.ngdc.noaa.gov/mgg/coastal/crm.html>.]

Settelmaier, J. B., A. Gibbs, P. Santos, T. Freeman, D. Gaer, 2011: Simulating Waves Nearshore (SWAN) Modeling Efforts at the National Weather Service (NWS) Southern Region (SR) Coastal Weather Forecast Offices (WFOs). Preprints, *24th Conference on Weather and Forecasting/20th Conference on Numerical Weather Prediction*, Seattle, WA, Amer. Meteor. Soc., P13A.4. [Available online at http://ams.confex.com/ams/91Annual/webprogram/Manuscript/Paper183540/Settelmaier_13A_4.pdf.]

The SWAN Team, cited 2010a: SWAN Model Page. [Available online at: <http://swanmodel.sourceforge.net/>]

The SWAN Team, cited 2010b: User Manual SWAN Cycle III Version 40.81. Available online at http://swanmodel.sourceforge.net/online_doc/swanuse/swanuse.html

Tolman, H.L., 2002: Limiters in third-generation wind wave models. *Global Atmos. and Ocean. System*, **8**, 67-83.

WAMDI Group, 1988. The WAM model—a third generation ocean wave prediction model. *J. Phys. Oceanogr.*, **18**, 1775-1810.

Zijlema, M., and A. J. van der Westhuysen, 2005: On convergence behavior and numerical accuracy in stationary SWAN simulations of nearshore wind wave spectra. *Coastal Engineering*, **52**, 237–256.

Region Information Technology Officer (ITO). Without Doug’s technical skills and dedicated work to these projects they would not have advanced as far as they have.

6. ACKNOWLEDGEMENTS

The authors like to acknowledge the enormous contribution to the NWSSR SWAN and National NWPS projects of Douglas Gaer, NWS Southern